applied sciences

MDPI

Article

Smart Devices Based on the Soft Actuator with Nafion-Polypropylene-PDMS/Graphite Multilayer Structure

Yao Wei, Shihao Li, Xiaofan Zhang, Yanjun Fu and Kejian Chen *

Shanghai Key Lab of Modern Optical System, Engineering Research Center of Optical Instrument and System of the Ministry of Education, School of Optical-Electrical and Computer Engineering, University of Shanghai for Science and Technology, 516 Jungong Road, Shanghai 200093, China; weiyao2024@163.com (Y.W.); work.lish@gmail.com (S.L.); 19921895461@163.com (X.Z.); 18351923105@163.com (Y.F.)

* Correspondence: ee.kjchen@gmail.com

Received: 11 February 2020; Accepted: 3 March 2020; Published: 6 March 2020

Featured Application: This stimulus-driven, fast-response and large-scale deformation flexible actuator provides a new alternative for bionic application, artificial skin, and soft sensor development.

Abstract: The demand for multi-functional soft actuators with simple fabrication and fast response to multiple stimuli is increasing in the field of smart devices. However, for existing actuators that respond to a single stimulus, it is difficult to meet the requirements of application diversity. Herein, a type of multi-stimulus responsive soft actuator based on the Nafion-Polypropylene-polydimethylsiloxane (PDMS)/Graphite multilayer membranes is proposed. Such actuators have an excellent reversible response to optical/thermal and humidity stimulation, which can reach a 224.56° bending angle in a relative humidity of 95% within 5 s and a maximum bending angle of 324.65° in 31 s when the platform temperature is 80 °C, and has a faster response (<0.5 s) to optical stimuli, as an asymmetric structure allows it to bend in both directions. Based on such an actuator, some applications like flexible grippers and switches to carry items or control circuits, bionic flytraps to capture and release "prey", have also been developed and studied. These provide potential applications in the fields of soft sensors, artificial skin and flexible robots.

Keywords: Nafion; Bionic actuator; Smart materials; Graphite; humidity response; optical response

1. Introduction

In recent years, the demand for smart actuators based on flexible intelligent driving materials has increased [1–4]. The role of flexible intelligent driving materials is to convert external stimuli (such as light, heat, humidity, magnetic field/electric field) into executable actions or signals needed by processors through rapid, reversible and controllable structural/morphological changes [5–16]. Flexible smart actuators driven by these stimuli have significant advantages in the soft robot, electronic skin, bionic technology and other fields [17–20]. For example, inspired by the flicking finger motions for rapidly releasing elastic energy, a curled carbon nanotube (CNT)-polydimethylsiloxane (PDMS) bilayer composite film actuator was designed and fabricated to simulate gymnastics tumbling in the air under low voltage and light illumination [21]. The flexible material encapsulates the micro-fabricated gold skeleton to replicate the fish's morphology, driving the fish's swimming and steering with optical stimulation [22]. Reversible deformed graphene monolayer paper combined with polyvinylidene fluoride (PVDF) film can stretch the PVDF film under light stimulation and produce open-circuit voltage up to 4 V [23]. However, most flexible actuators have restrictions such as single stimulation,

slow response and recovery. It is desirable to develop a kind of actuator with advantages such as multiple stimulus-driven, fast-response and large-scale deformation for the multifunctional devices.

The flexible polymer Nafion has high ionic conductivity, and is commonly used to make ion exchanged membranes for chlorine gas and alkali production, as well as for proton exchanged membranes in fuel cell polymer electrodes [24,25]. However, the sulfonic acid groups in Nafion are highly hydrating, absorb water and swell very quickly and efficiently, and the intrinsic connection of sulfonic acid groups allows water to be removed quickly. Hence, the Nafion film has emerged as an interesting candidate component for an actuator which exhibits fast response and large-scale deformation under varying humidity [26]. PDMS, a transparent non-toxic organic polymer material, has a high thermal expansion coefficient and excellent biocompatibility and hydrophobicity, good chemical stability and commercial availability; these characteristics make it often and preferrably used in flexible actuators, sensors, biomechanical systems, microfluidic systems, etc. [27–31]. Also, traditional carbon-based material graphite has become a popular actuator component due to its excellent optical, thermal, electrical and mechanical properties. It is able to convert light into heat effectively because it can strongly absorb a wide range of light from ultraviolet to near infrared (NIR) wavelengths [32–35].

Thus, a new type soft actuator composed of Nafion-polypropylene-PDMS/Graphite is proposed in this paper. The actuator has an excellent reversible response to humidity, optical and thermal stimulation, as shown in Figure 1a. The humidity-driven actuation is due to the hygroscopic property of the Nafion layer and the non-hygroscopic property of PDMS/Graphite. Once the relative humidity increased, the absorption of water molecules resulted in the swelling of Nafion, while PDMS/Graphite layer remained substantially, so the actuator bent towards the PDMS/Graphite side [36,37]. The light-driven and thermal-driven actuations are a utilization of difference of thermal expansion coefficient between PDMS/Graphite and Nafion layer. Also, graphite is able to convert photonic energy into thermal energy, which can speed up the volume expansion of PDMS/Graphite [38–41]. Meanwhile, the increase of temperature also leads to water desorption and shrinking of the Nafion layer. Hence, the actuator has an extraordinary bending response to the Nafion side, and several smart devices based on it have been demonstrated to be effective; thus, the soft actuator will have potential applications in bioinspired applications, soft robots and so on.

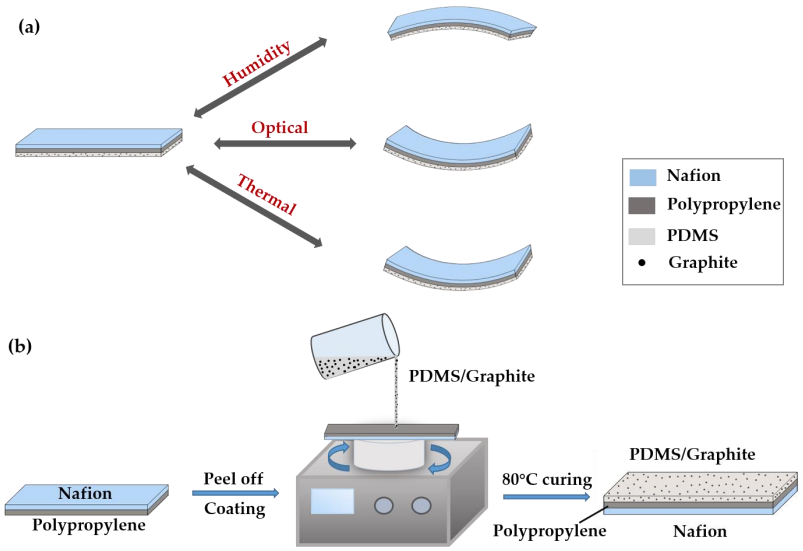

Figure 1. (**a**) Schematic diagram of multilayer membrane response to humidity, optical and thermal stimulation. (**b**) Schematic illustration of the fabrication of Nafion-polypropylene-PDMS/Graphite multilayer membrane actuator.

2. Materials and Methods

2.1. Materials

Nafion N211 (17.78 μm) and polypropylene (25.4 μm) composite film was commercially purchased from Kunshan Yi Erwei International Trade Co., Ltd., Kunshan, China. PDMS was obtained from Huishan Bihui Electronic Products Co., Ltd., Wuxi, China (Sylagrd 184 silicone elastomer, Dow Corning, Midland, Michigan, USA), graphite particle (800 nm) was provided by Dongguan xieli Co., Ltd., Dongguan, China. Infrared bulb (100 W, Philips E27) that provided NIR light source, was commercially purchased from Shenzhen Dazhongyu Runxiang E-Commerce Co., Ltd., Shenzhen, China.

2.2. Fabrication and Measurement of the Multilayer Membrane-Based Actuator

The preparation process of the stimuli-responsive actuator can be seen in Figure 1b; PDMS was comprised of A (silicone elastomer liquid base) and B (curing agent) viscous liquid components. Initially, N-hexane was added into A (silicone elastomer liquid base) for dilution with a weight ratio of 3:10 and stirred vigorously for 5 min. Then, graphite particles were appended to A (silicone elastomer liquid base) with a weight ratio of 1.5:10 and mixed for 5 min. Next, the viscose solution was degassed in a conditioning mixer (THINKY AR-100) after adding B (curing agent) into A (silicone elastomer liquid base) and thoroughly mixed (A:B = 10:1). After cleaning work, Nafion and polypropylene films that had been stuck together were stripped from the purchased composite film, and cropped into a suitable size and then attached to the slide. Then, the viscous PDMS mixture was coated onto Nafion film on slide substrate by the spin-coating method (Rotation speed: 2000 r/min for 20 s) and cured in the oven at a temperature of 80 °C for 2 h. Finally, the multilayer membrane was cooled and carefully peeled from the substrate for further use.

The water contact angle (CA) was measured using a Contact Angle Meter DSA30S (KRUSS. Germany). The sample was cut into a size of 0.5 cm × 1 cm, and pasted on the slide with double-sided adhesive, then the CA analyzer was used to drop 1 mL deionized water into the sample, measured the CA between the water drop and the film to analyze the hydrophilicity of the film. The actuation performance is measured by the image processing software Picpick, which is automatically accurate angle to two decimal places. The entire testing process was recorded, and then the software Picpick was used to measure the bending angle of the sample at each moment in the response process.

3. Results and Discussion

3.1. Multilayer Membrane of Humidity Responsive Deforming

Due to the polymer chain in Nafion, it can rapidly exchange with water and form a large number of water transport channels. As the humidity increases, Nafion absorbs moisture and swells very quickly and efficiently, and moisture can be quickly removed because of the intrinsic connection of sulfonic acid groups when humidity is reduced [42,43]. As shown in Figure 2a, once the relative humidity in the box was increased, Nafion layer absorbed moisture and swelled, while the middle polypropylene layer and the PDMS/Graphite layer remained substantially as a hydrophobic layer, so the multilayer membrane bent toward the PDMS/Graphite side, as shown in Figure 2b. Moreover, Figure 2c,d illustrate the Nafion film exhibits a water CA of 79.97°, which is less than that of mixed PDMS/Graphite layer (123.64°), this obvious difference in hydrophilicity causes asymmetric deformation of the multilayer membrane when the ambient humidity changes. When the humidity was lowered, the Nafion layer lost water and shrank, so the multilayer membrane returned to its original state under the elastic recovery force of the polypropylene layer and the PDMS/Graphite layer. Figure 2e shows the rising tendency of the maximum bending angles of the multilayer membrane with the humidity increasing from 30% to 95%. Furthermore, Figure 2f illustrates the multilayer membrane reached its maximum bending angle of 224.56° within 5 s under conditions of 95% humidity. This fast, large-scale response

to moisture and recovery characteristics indicates the multilayer membranes have great potential applications in an environment of varied humidity.

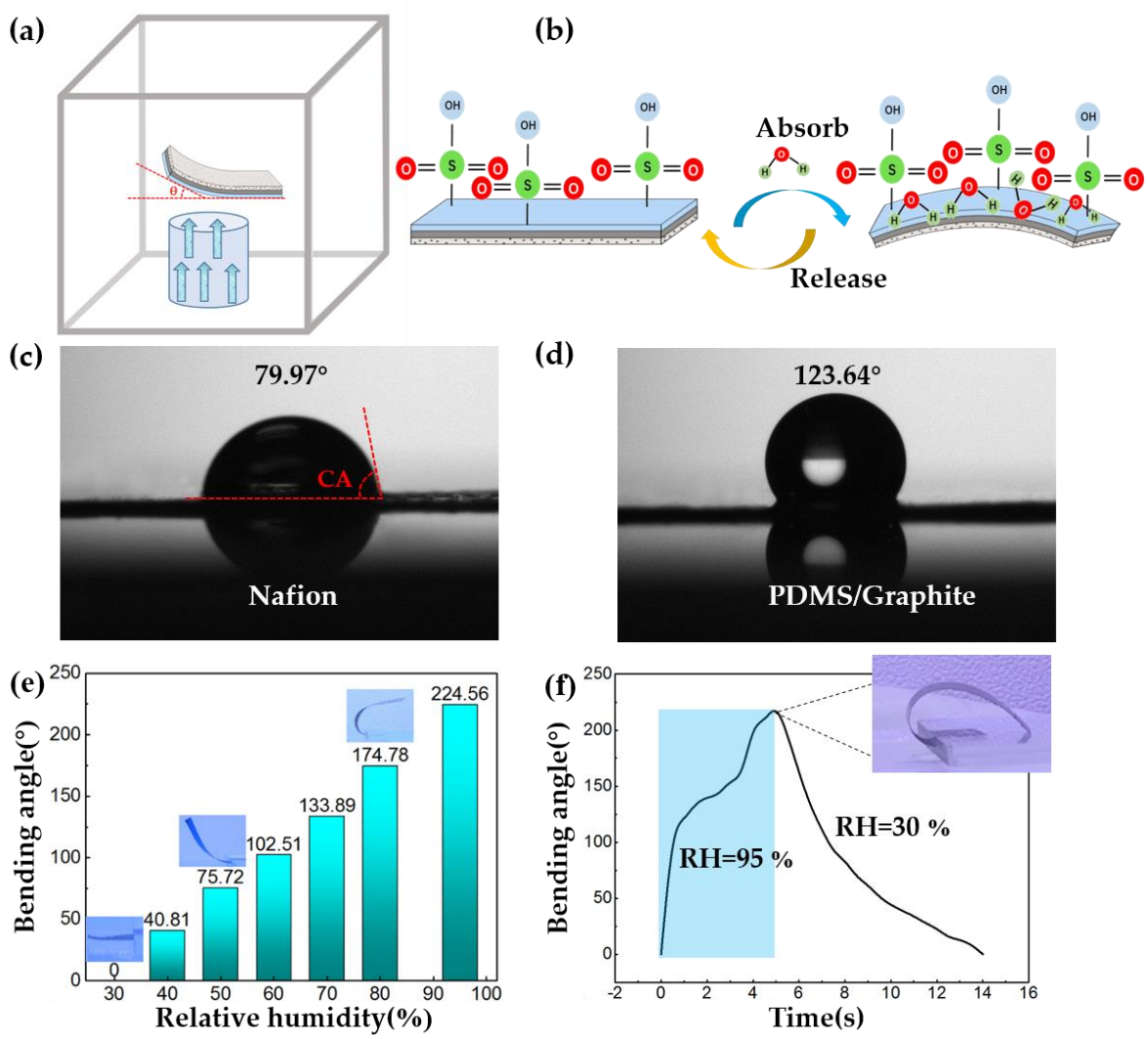

Figure 2. Humidity-responsive behavior of the multilayer membrane (the test ambient temperature was 25 °C). (**a**) Schematic diagram of the humidity deformation response testing. (**b**) Schematic illustration of the reversible deformation behaviors when humidity changes. (**c**) Photo of water droplet CA for Nafion film and (**d**) PDMS/Graphite film. (**e**) The maximum bending angle of the multilayer membrane under different relative humidity. (**f**) The time-dependent bending angle of the multilayer membrane under 95% (blue area) and 30% humidity stimulation.

3.2. Multilayer Membrane of Optical Responsive Deforming

To enable the multilayer membrane to respond to a wider range of electromagnetic spectrum, graphite was selected as a light-absorbing material because of its broad-spectrum absorption properties. The SEM image of the multilayer membrane's cross-section in Figure 3a shows that in the layered structure, graphite particles are uniformly dispersed in the PDMS layer, which is helpful to transfer the photothermal more quickly and evenly. When the multilayer membrane was illuminated, the PDMS/Graphite layer absorbed light efficiently, and the volume of the PDMS/Graphite layer began to expand. Simultaneously, the NIR light will also made the ambient temperature around the membrane rise and caused the local humidity to decrease, which finally led to the shrink of the Nafion layer by losing water which enhances the bending tendency towards the Nafion layer as illustrated in Figure 3b. When the light disappeared, the graphite particles began to dissipate heat. The PDMS/Graphite layer

began to return to its original state, and then the multilayer membrane returned to its original state quickly. At the same time, local humidity around the membrane increased rapidly to the level of environment humidity after the light off, and the Nafion layer began to absorb moisture and swelled, which enhanced the expanding tendency of the device towards the PDMS/Graphite side.

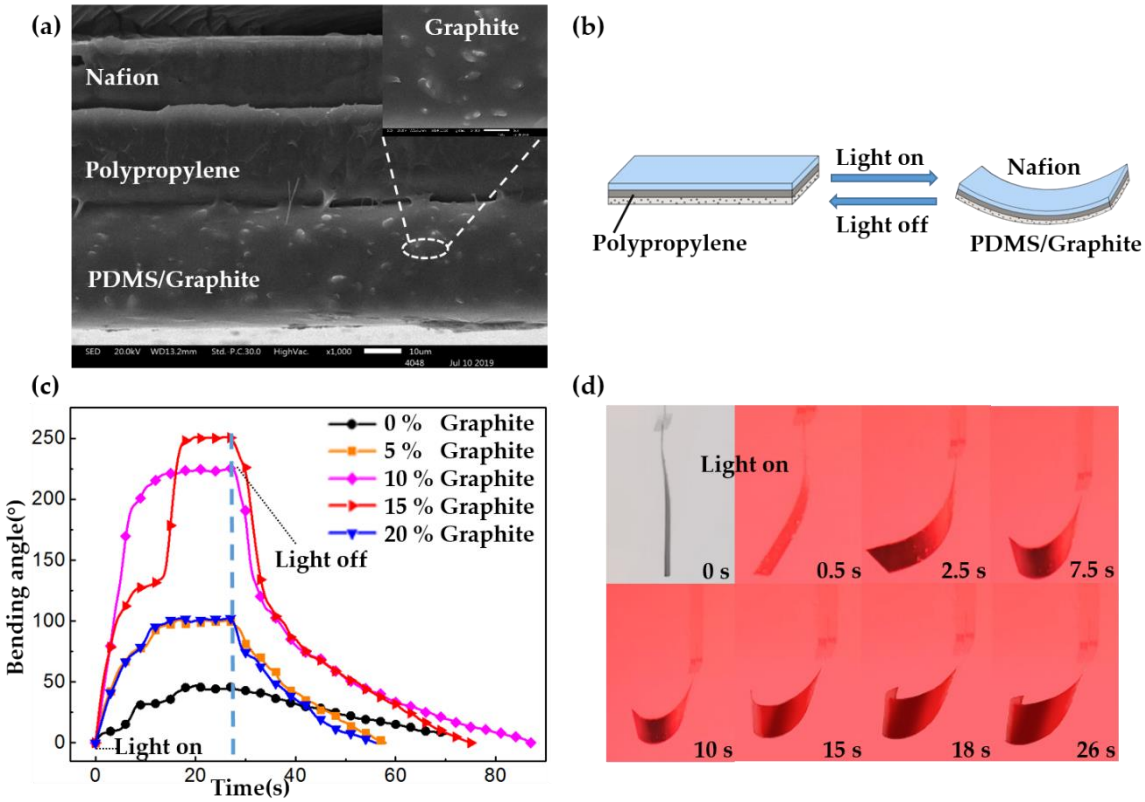

Figure 3. Optical-responsive behavior of the multilayer membrane (the test ambient relative humidity was 30%). (**a**) SEM image of the cross-section of the Nafion-polypropylene-PDMS/Graphite multilayer membrane. (**b**) Schematic illustration of the reversible deformation behaviors under illumination. (**c**) Bending angle of the actuator with different graphite particle concentrations under the NIR light intensity of 0.88 W·cm^{-2}. (**d**) Real-time process of light response of the multilayer membrane with 15% graphite concentration.

For the purpose of investigating the effect of the light absorption efficiency on the deformation of the multilayer membrane under illumination, we changed the graphite concentrations (0%, 5%, 10%, 15%, 20%) in the PDMS layer, as shown in Figure 3c. Under the same NIR light intensity of 0.88 W·cm^{-2}, the sample with 0% graphite concentration needed the longest time to reach its peak bending angle 47.64° within 20 s, which means its photothermal conversion efficiency is the lowest. When the graphite concentrations increased, the maximum bending angle and response speed of the multilayer membrane also rose. When the graphite concentration was 15%, the multilayer membrane could quickly reach its maximum bending angle of 251.97°. However, it is worth noting that when the graphite concentration rose to 20%, the stress of the multilayer membrane increased and the strain decreased, resulting in a decrease of multilayer membrane in responding speed and the maximum bending angle. Although the photothermal conversion efficiency of the multilayer membrane benefits from the increase of the graphite concentrations, the bending trend is limited by the flexibility of the device as well. Within a certain range, in order to obtain the best overall response, a multilayer membrane with a graphite concentration of 15% was selected for further use. Figure 3d shows the response process of the multilayer membrane with 15% graphite concentration under NIR light intensity of 0.88 W·cm^{-2}.

3.3. Multilayer Membrane of Thermal Responsive Deforming

The principle of the multilayer membrane's deformation when the temperature rises is similar to the optical response deformation. The PDMS/Graphite layer with a large thermal expansion coefficient expanded after being heated, the Nafion layer shrank due to water loss, and the middle layer remained unchanged. Due to asymmetric deformation, it caused the membrane to bend towards the Nafion side. During the temperature test, once the multilayer membrane began to gradually deviate from the heating platform, the multilayer membrane was mainly heated by the air between the multilayer membrane and the heating platform. As shown in Figure 4a, when the temperature of the heating platform was between 30 °C and 80 °C, the maximum bending angle of the multilayer membrane increased with increasing temperature.

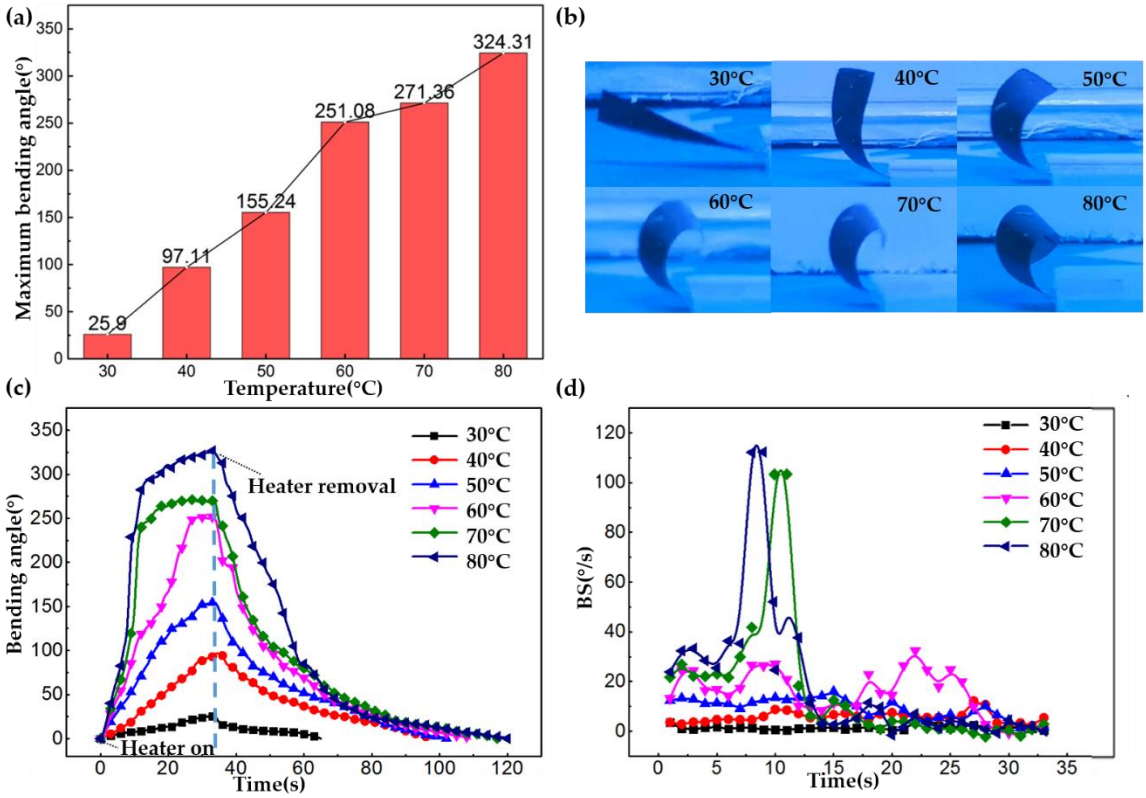

Figure 4. Thermal-responsive behavior of the multilayer membrane (test ambient relative humidity was 30%). (**a**) The maximum bending angle of multilayer membrane upon various temperatures. (**b**) Bending images of the multilayer membrane under different temperatures. (**c**) Bending angle of the multilayer membrane with 15% graphite particle concentrations upon various temperatures. (**d**) Schematic diagram of the multilayer membrane's BS.

Figure 4b shows bending images of the actuator under different temperatures, when the platform temperature is 80 °C, the multilayer film can reach a maximum bending angle of 324.65° in 31 s. Such large-scale deformation can meet the stimulation response requirements of most scenes. Figure 4c shows the bending angle of the actuator with 15% graphite particle concentrations upon various temperatures, and as the bending angle became larger, we could use the bending speed (BS) to characterize the process before the bending angle of the multilayer membrane reached the peak. The bending angle (BA) increases with time (T), the increased bending angle (ΔBA) and time interval (ΔT) can be used to indicate BS, BS = ΔBA/ΔT, as shown in Figure 4d; the illustrated bending speed BS decreases with time, which indicates the rate of thermal conversion decrease, and the efficiency of heating by air is lower than heating through the platform directly.

4. Multiple Stimulus-Driven Smart Devices

Multilayer membranes experience a rapid and large-scale deformation under a variety of stimuli, making them a basis for actuators with multiple functions. As a simple example of application, we designed a flexible gripper possessing a multilayer film with a graphite concentration of 15%. The switching of the NIR light was controlled so that the multilayer membrane gripper could achieve the action of grabbing-releasing objects. As shown in Figure 5a–d, in a normal environment with a humidity of 35%, the simple gripper was controlled to grab foam cubes and transport them to the shelf under the illumination. Furthermore, in order to test the grasping ability of the gripper on irregularly shaped objects, medicinal capsules (0.06 g) were used as transport objects; Figure 5e–h show the ability of the gripper to pick and release capsules, indicating that the multilayer membrane will have potential applications in areas such as fragile items and drug delivery. Also, because the multilayer membrane has different bending directions under different stimuli, a single-pole double-throw switch based on the multilayer membrane was fabricated. As shown in Figure 6a,d, the circuit where the membrane was located serves as an input channel. When the ambient humidity rose to 70%, Figure 6b,c show the membrane bent upward, the input signal was calculated by the microprocessor, the microprocessor output lighted up the blue Light Emitting Diode (LED), and the Liquid Crystal Display (LCD) displayed "Moist, Moist!". On the contrary, when the NIR light illuminated the switch, Figure 6e–f show the membrane bent downward to light the red LED, and the LCD displayed "Hot, Hot !". This provides good inspiration for us to develop flexible sensors.

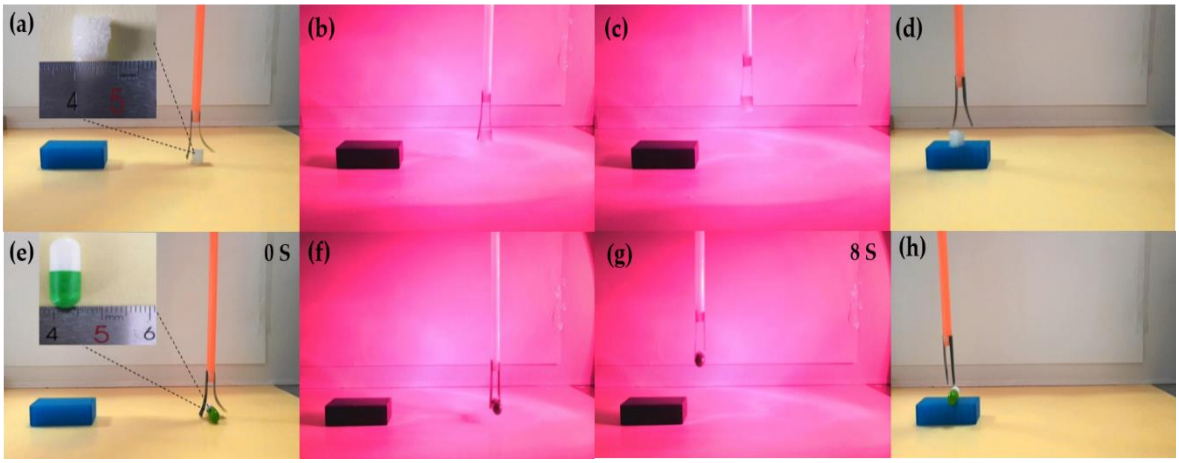

Figure 5. Optical-responsive flexible gripper. (**a**–**d**) Images showing a multilayered membrane-based gripper driven by infrared light to grab and transported foam cubes. (**e**–**h**) Gripper transfer medicinal capsules (0.06 g) in 11 s.

Inspired by the Venus flytrap, which can control-blade opening and closing, membrane actuators can be also applied to biomimetic devices, as shown in Figure 7a,b, a bionic flytrap was fabricated to achieve the function of prey capture and release. Figure 7c shows the schematic diagram of the proposed bionic flytrap with the multiple stimulus-driven membrane, and wipe papers (KIMTECH34155) have been adopted to absorb moisture (or water) from "prey" and worked as the trigger sensor. The ambient humidity around the actuator will be increased fast by the wetted wipe paper and finally trigger the actuator to bend towards the center and catch "prey". Figure 7d–f show the capturing process that a "prey" (wet paper ball) fell into the bionic trap and was gradually captured. The grasping performance of the bionic trap is also verified in Figure 7g by flipping the whole device. The paper ball was wrapped up well, which means the "prey" was captured and locked by the bionic flytrap. It should be noted that the "prey" paper ball could not fall off until the ambient humidity around the actuator decreases to a certain low level of humidity and was not strong enough for bionic flytrap to keep the "prey". As the bionic flytrap was manufactured with the multiple stimulus-driven membrane, one can speed

up the process and release the "prey" immediately by illuminating the bionic flytrap with infrared light, as shown in the inset of Figure 7g.

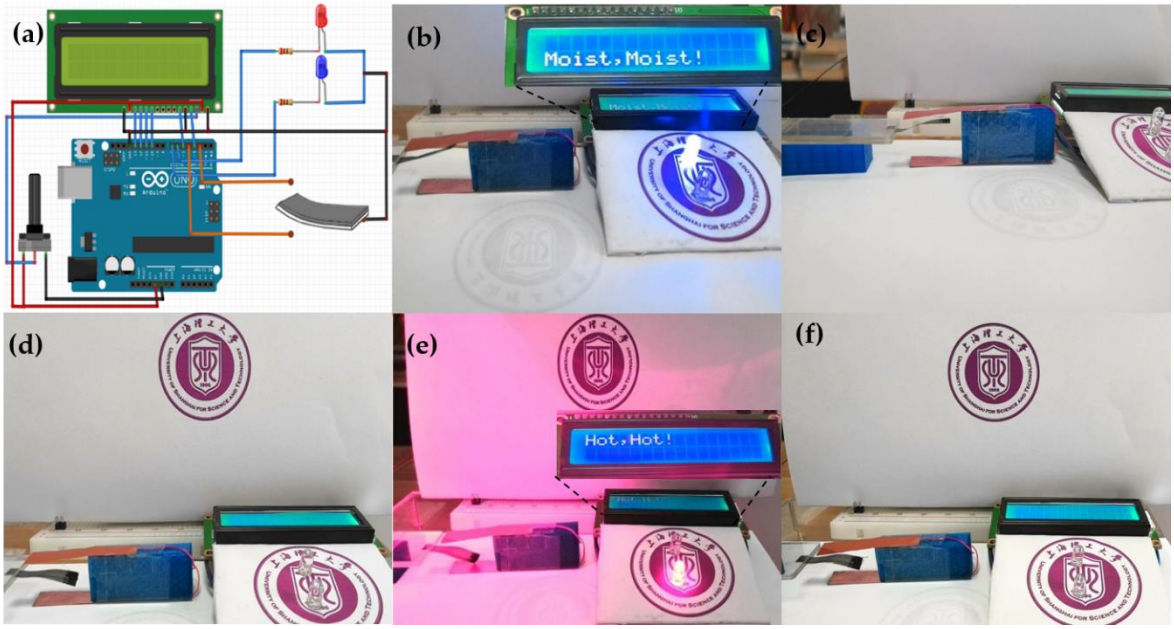

Figure 6. Optical and humidity-responsive switches. (**a**) Schematic of the membrane-based switch circuit. (**b**–**c**) The response of LED and LCD in a humid environment. (**d**) The original state of the switch based on actuator in the circuit. (**e**–**f**) The response of LED and LCD in the photothermal environment.

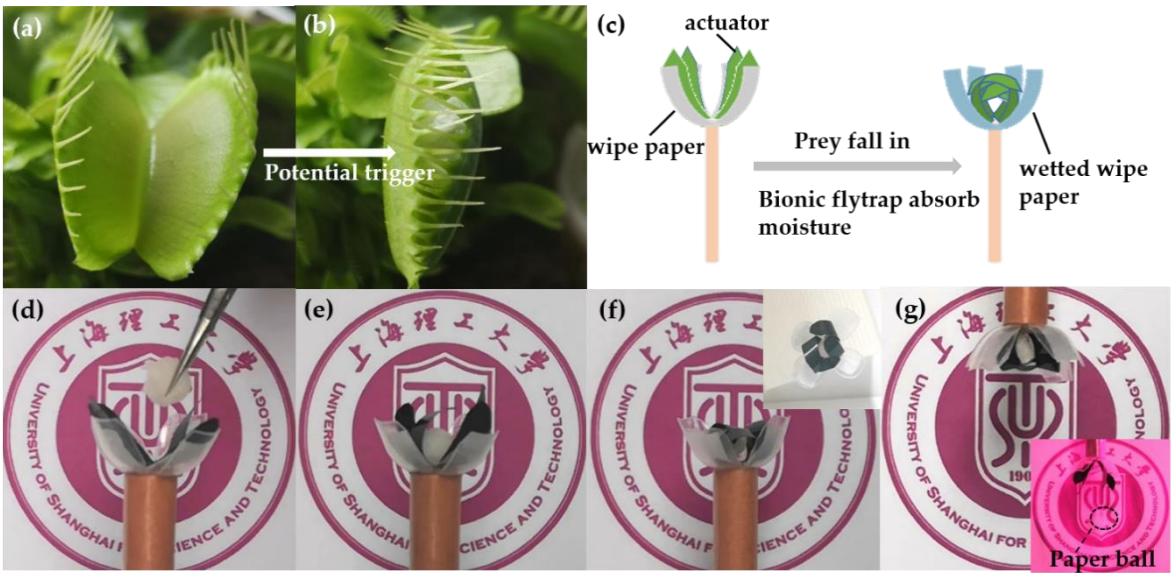

Figure 7. Bionic flytrap. (**a**–**b**) Schematic diagram of a flytrap in its open and closed state. (**c**) Schematic illustration of the structure and operation principle of bionic flytrap. (**d**–**f**) The process of bionic flytrap captured a wet paper ball and top view of bionic flytrap. (**g**) Bionic flytrap in inverted place and released "prey" paper ball under high energy infrared light.

5. Conclusions

In summary, a multi-stimulus response soft actuator was fabricated with multilayer membrane (Nafion-Polypropylene-PDMS/Graphite). This soft actuator exhibits rapidly reversible bending in

a humid environment or under optical/thermal conditions, and the asymmetric structure enables it to bend in both directions. When the graphite concentration is 15%, the soft actuator has a faster response (<0.5 s) to optical stimuli. Also, it can reach a maximum bending angle of 324.65° in 31 s when the platform temperature is 80 °C and reach a 224.56° bending angle in a relative humidity of 95% within 5 s. Furthermore, smart devices that designed and prepared based on the soft actuator, such as light-controlled grippers, light/humidity-driven switches, and the bionic flytrap, have also been demonstrated in this paper. This stimulus-driven, fast-response and large-scale deformation flexible actuator provides a new alternative for bionic application, artificial skin and soft sensor development.

Author Contributions: Conceptualization, Y.W.; methodology, YW., S.L.; formal analysis, Y.W.; investigation, S.L.; data curation, Y.W.; writing—original draft preparation, Y.W.; writing—review and editing, K.C., Y.F., X.Z.; visualization, X.Z.; supervision, K.C.; All authors have read and agreed to the published version of the manuscript.

Funding: This research was funded by National Natural Science Foundation of China, grant number 61205095 and Shanghai Young College Teacher Develop funding schemes, grant number slg11006.

Conflicts of Interest: The authors declare no conflict of interest. The funders had no role in the design of the study; in the collection, analyses, or interpretation of data; in the writing of the manuscript, or in the decision to publish the results.

References

1. Kim, S.; Laschi, C.; Trimmer, B. Soft robotics: A bioinspired evolution in robotics. *Trends Biotechnol.* **2013**, *31*, 287–294. [CrossRef] [PubMed]
2. Ma, M.; Guo, L.; Anderson, D.G.; Langer, R. Bio-inspired polymer composite actuator and generator driven by water gradients. *Science* **2013**, *339*, 186–189. [CrossRef]
3. Park, S.; An, J.; Suk, J.W.; Ruoff, R.S. Graphene-based actuators. *Small* **2010**, *6*, 210–212. [CrossRef] [PubMed]
4. Stuart, M.A.; Huck, W.T.; Genzer, J.; Muller, M.; Ober, C.; Stamm, M.; Sukhorukov, G.B.; Szleifer, I.; Tsukruk, V.V.; Urban, M.; et al. Emerging applications of stimuli-responsive polymer materials. *Nat. Mater.* **2010**, *9*, 101–113. [CrossRef] [PubMed]
5. Hu, Y.; Wu, G.; Lan, T.; Zhao, J.; Liu, Y.; Chen, W. A Graphene-Based bimorph structure for design of high performance photoactuators. *Adv. Mater.* **2015**, *27*, 7867–7873. [CrossRef] [PubMed]
6. Cheng, H.; Zhao, F.; Xue, J.; Shi, G.; Jiang, L.; Qu, L. One single graphene oxide film for responsive actuation. *ACS Nano* **2016**, *10*, 9529–9535. [CrossRef]
7. Lum, G.Z.; Ye, Z.; Dong, X.; Marvi, H.; Erin, O.; Hu, W.; Sitti, M. Shape-programmable magnetic soft matter. *Proc. Natl. Acad. Sci. USA* **2016**, *113*, E6007–E6015. [CrossRef]
8. Shen, Q.; Trabia, S.; Stalbaum, T.; Palmre, V.; Kim, K.; Oh, I.K. A multiple-shape memory polymermetal composite actuator capable of programmable control, creating complex 3D motion of bending, twisting, and oscillation. *Sci. Rep.* **2016**, *6*, 24462. [CrossRef]
9. Chen, L.; Weng, M.; Zhou, P.; Zhang, L.; Huang, Z.; Zhang, W. Multi-responsive actuators based on a graphene oxide composite: Intelligent robot and bioinspired applications. *Nanoscale* **2017**, *9*, 9825–9833. [CrossRef]
10. Sang, W.; Zhao, L.; Tang, R.; Wu, Y.; Zhu, C.; Liu, J. Electrothermal actuator on graphene bilayer film. *Macromol. Mater. Eng.* **2017**, *302*, 1700239. [CrossRef]
11. Zhang, L.; Qiu, X.; Yuan, Y.; Zhang, T. Humidity- and sunlight-driven motion of chemically bonded polymer bilayer with programmable surface patterns. *ACS Appl Mater Interfaces* **2017**, *9*, 41599–41606. [CrossRef] [PubMed]
12. Ge, Y.; Cao, R.; Ye, S.; Chen, Z.; Zhu, Z.; Tu, Y.; Ge, D.; Yang, X. A bio-inspired homogeneous graphene oxide actuator driven by moisture gradients. *Chem. Commun. (Camb.)* **2018**, *54*, 3126–3129. [CrossRef] [PubMed]
13. Kim, Y.; Yuk, H.; Zhao, R.; Chester, S.A.; Zhao, X. Printing ferromagnetic domains for untethered fast-transforming soft materials. *Nature* **2018**, *558*, 274–279. [CrossRef] [PubMed]
14. Ni, Y.; Chen, K.; Long, K.; Ji, R.; Hua, Y.; Zhang, X.; Fu, Y.; Wei, Y.; Zhuang, S. The fabrication of optical and magnetic responsive deforming multilayered film. *J. Appl. Polym. Sci.* **2018**, *135*, 46884. [CrossRef]
15. Zhou, J.; Wu, C.; Wu, D.; Wang, Q.; Chen, Y. Humidity-sensitive polymer xerogel actuators prepared by biaxial pre-stretching and drying. *Chem. Commun. (Camb.)* **2018**, *54*, 11610–11613. [CrossRef]

16. Wani, O.M.; Verpaalen, R.; Zeng, H.; Priimagi, A.; Schenning, A. An artificial nocturnal flower via humidity-gated photoactuation in liquid crystal networks. *Adv. Mater.* **2019**, *31*, e1805985. [CrossRef]
17. Heibeck, F.; Tome, B.; Della Silva, C.; Ishii, H. uniMorph: Fabricating thin-film composites for shape-changing interfaces. In Proceedings of the 28th Annual ACM Symposium on User Interface Software and Technology (UIST), Charlotte, NC, USA, 8–11 November 2015; pp. 233–242.
18. Yao, L.; Ou, J.; Cheng, C.-Y.; Steiner, H.; Wang, W.; Wang, G.; Ishii, H. bioLogic: Natto cells as nanoactuators for shape changing interfaces. In Proceedings of the 33rd Annual CHI Conference on Human Factors in Computing Systems (CHI), Seoul, Korea, 18–23 April 2015; pp. 1–10.
19. Chortos, A.; Liu, J.; Bao, Z. Pursuing prosthetic electronic skin. *Nat Mater.* **2016**, *15*, 937–950. [CrossRef]
20. Wang, C.; Sim, K.; Chen, J.; Kim, H.; Rao, Z.; Li, Y.; Chen, W.; Song, J.; Verduzco, R.; Yu, C. Soft ultrathin electronics innervated adaptive fully soft robots. *Adv Mater.* **2018**, *30*, e1706695. [CrossRef]
21. Hu, Y.; Liu, J.; Chang, L.; Yang, L.; Xu, A.; Qi, K.; Lu, P.; Wu, G.; Chen, W.; Wu, Y. Electrically and sunlight-driven actuator with versatile biomimetic motions based on rolled carbon nanotube bilayer composite. *Adv. Funct. Mater.* **2017**, *27*, 1704388. [CrossRef]
22. Xiao, P.; Yi, N.; Zhang, T.; Huang, Y.; Chang, H.; Yang, Y.; Zhou, Y.; Chen, Y. Construction of a fish-like robot based on high performance graphene/PVDF bimorph actuation materials. *Adv. Sci. (Weinh.)* **2016**, *3*, 1500438. [CrossRef]
23. Mu, J.; Hou, C.; Zhu, B.; Wang, H.; Li, Y.; Zhang, Q. A multi-responsive water-driven actuator with instant and powerful performance for versatile applications. *Sci. Rep.* **2015**, *5*, 9503. [CrossRef] [PubMed]
24. Schmidt-Rohr, K.; Chen, Q. Parallel cylindrical water nanochannels in nafion fuel-cell membranes. *Nat. Mater.* **2008**, *7*, 75–83. [CrossRef] [PubMed]
25. Xie, T.; Li, J.; Zhao, Q. Hidden thermoreversible actuation behavior of nafion and its morphological origin. *Macromolecules* **2014**, *47*, 1085–1089. [CrossRef]
26. Henkensmeier, D.; Gubler, L. Shape memory effect in radiation grafted ion exchange membranes. *J. Mater. Chem. A* **2014**, *2*, 9482–9485. [CrossRef]
27. Jung, T.; Yang, S. Highly stable liquid metal-based pressure sensor integrated with a microfluidic channel. *Sensors (Basel)* **2015**, *15*, 11823–11835. [CrossRef]
28. Jian, M.; Xia, K.; Wang, Q.; Yin, Z.; Wang, H.; Wang, C.; Xie, H.; Zhang, M.; Zhang, Y. Flexible and highly sensitive pressure sensors based on bionic hierarchical structures. *Adv. Funct. Mater.* **2017**, *27*, 1606066. [CrossRef]
29. Lee, D.W.; Park, J.S. Feasibility study of PDMS-based thermal microactuators. *Sensors Mater.* **2007**, *19*, 497–504.
30. Ishisaka, T.; Sato, H.; Akiyama, Y.; Furukawa, Y.; Morishima, K. Bio-actuated power generator using heart muscle cells on a PDMS membrane. In Proceedings of the TRANSDUCERS 2007—2007 International Solid-State Sensors Actuators and Microsystems Conference, Lyon, France, 10–14 June 2007; pp. 903–906.
31. Shankles, P.G.; Millet, L.J.; Ufrecht, J.A.; Retterer, S.T. Accessing microfluidics through feature-based design software for 3D printing. *PLoS ONE* **2018**, *13*, e0192752. [CrossRef]
32. Smausz, T.; Kondász, B.; Gera, T.; Ajtai, T.; Utry, N.; Pintér, M.; Kiss-Albert, G.; Budai, J.; Bozóki, Z.; Szabó, G.; et al. Determination of UV–visible–NIR absorption coefficient of graphite bulk using direct and indirect methods. *Appl. Phys. A* **2017**, *123*, 633. [CrossRef]
33. Weng, M.; Zhou, P.; Chen, L.; Zhang, L.; Zhang, W.; Huang, Z.; Liu, C.; Fan, S. Multiresponsive bidirectional bending actuators fabricated by a pencil-on-paper method. *Adv. Funct. Mater.* **2016**, *26*, 7244–7253. [CrossRef]
34. Kurra, N.; Kulkarni, G.U. Pencil-on-paper: Electronic devices. *Lab Chip* **2013**, *13*, 2866–2873. [CrossRef] [PubMed]
35. Yang, L.; Qi, K.; Chang, L.; Xu, A.; Hu, Y.; Zhai, H.; Lu, P. Powerfully dual-responsive soft actuator and photo-to-electric generator based on graphene micro-gasbags for bioinspired applications. *J. Mater. Chem. B* **2018**, *6*, 5031–5038. [CrossRef]
36. Zhong, Y.; Zhang, F.; Wang, M.; Gardner, C.J.; Kim, G.; Liu, Y.; Leng, J.; Jin, S.; Chen, R. Reversible humidity sensitive clothing for personal thermoregulation. *Sci. Rep.* **2017**, *7*, 44208. [CrossRef] [PubMed]
37. Bauer, F.; Denneler, S.; Willert-Porada, M. Influence of temperature and humidity on the mechanical properties of Nafion® 117 polymer electrolyte membrane. *J. Polym. Sci. Part B Polym. Phys.* **2005**, *43*, 786–795. [CrossRef]

38. Jiang, W.; Niu, D.; Liu, H.; Wang, C.; Zhao, T.; Yin, L.; Shi, Y.; Chen, B.; Ding, Y.; Lu, B. Photoresponsive soft-robotic platform: Biomimetic fabrication and remote actuation. *Adv. Funct. Mater.* **2014**, *24*, 7598–7604. [CrossRef]
39. Jiang, S.; Guo, W.; Liu, S.; Huang, X.; Li, Y.; Li, Z.; Wu, H.; Yin, Z. Grab and heat: Highly responsive and shape adaptive soft robotic heaters for effective heating of objects of three-dimensional curvilinear surfaces. *ACS Appl. Mater. Interfaces* **2019**, *11*, 47476–47484. [CrossRef]
40. Seo, D.K.; Kang, T.J.; Kim, D.W.; Kim, Y.H. Twistable and bendable actuator: A CNT/polymer sandwich structure driven by thermal gradient. *Nanotechnology* **2012**, *23*, 075501. [CrossRef]
41. Tang, R.; Sang, W.; Wu, Y.; Zhu, C.; Liu, J. Multi-wavelength light drivable oscillatory actuator on graphene-based bilayer film. *Macromol. Mater. Eng.* **2017**, *302*, 1600384. [CrossRef]
42. Gebel, G. Structural evolution of water swollen perfluorosulfonated ionomers from dry membrane to solution. *Polymer* **2000**, *41*, 5829–5838. [CrossRef]
43. Hwang, G.S.; Parkinson, D.Y.; Kusoglu, A.; MacDowell, A.A.; Weber, A.Z. Understanding water uptake and transport in nafion using X ray microtomography. *ACS Macro Lett.* **2013**, *2*, 288–291. [CrossRef]

© 2020 by the authors. Licensee MDPI, Basel, Switzerland. This article is an open access article distributed under the terms and conditions of the Creative Commons Attribution (CC BY) license (http://creativecommons.org/licenses/by/4.0/).